An Illumination Model for a System of Isotropic Substrate- Isotropic Thin Film with Identical Rough Boundaries

Isabelle Icart, Didier Arquès
(icart@univ-mlv.fr, arques@univ-mlv.fr)
Université de Marne-La-Vallée
5, boulevard Descartes, Champs-sur-Marne, F-77454 Marne-La-Vallée CEDEX 2

Abstract. A new physically-based illumination model describing the interaction of light with a system composed of an isotropic substrate coated by an isotropic film with geometrically identical statistical rough boundaries (ITF) is presented. This model divides the intensity reflected from the system into three components: specular, directional-diffuse and uniform diffuse intensity. The formulas for the intensity reflected coherently (specular) and incoherently (directional-diffuse) from the system are derived within the framework of the scalar diffraction theory. Assuming that the slopes on the boundaries of the film are small, a first-order expansion of the reflection coefficient is used in the evaluation of the Helmholtz-Kirchhoff integral which allows to calculate the previous intensities. The consistency of the model is evaluated numerically and appraised visually by comparison with classic approximations.

1 Introduction

In the real world all materials are not polished nor perfectly smooth (soap films are an example of surfaces that can be considered as perfectly smooth [10]): the surfaces are assumed to be a collection of irregularities which scatters light into various directions, though certain directions are privileged. A smooth surface will reflect light only in the specular direction whereas a rough surface (roughness is a non intrinsic property which depends on wavelength and incidence angle - see e.g. the Rayleigh criterion [2] p.10) will show a diffuse-like behaviour due to diffraction by these irregularities. The results of Beckmann and Spizzichino [1] in physical optics, which gave rise to the illumination model of Cook and Torrance [5] and later to the more complete model of He, Torrance, Sillion and Greenberg [8] in computer graphics deal with calculating the coherent (specular) and incoherent (directional-diffuse) components of light diffracted by a single rough surface with uniform reflection coefficient. The problem of rendering systems consisting of rough thin films or rough multilayers is more complex because the reflection coefficient of such systems depends on the geometry (and then on the roughness) of each boundary and cannot be considered as uniform. People already achieved realistic pictures of rough thin films or multilayers by means of spectral BRDFs [7] or intuitive approaches (see e.g. [15] and [6]) coupled with classic illumination models. In 1994, Callet [3] obtained pictures of thin film coatings and metallic paints by means of the geometric optics model of Cook and Torrance [5] used together with some approximations. These approximations consist in calculating the bidirectional reflectance function for each boundary and using the interference formula valid for smooth films (see formula (1)) to deduce the total BRDF of the system (see [4] p. 203-205). Within

the framework of the scalar diffraction theories, it is nevertheless possible to determine precisely (or at least with a given accuracy) the components of light reflected towards an observer from a system substrate-thin film under certain assumptions. In this paper, we first evaluate the coherent and incoherent intensities reflected from a system substrate-identical thin film towards an observer situated in the Fraunhofer diffraction zone ([2] p. 343), in a given direction. Then, we deduce the local illumination model as a sum of three intensities : specular, directional-diffuse and uniform diffuse. These results will be compared with those obtained by neglecting the spatial dependence of the reflection coefficient (which amounts to considering the system as an equivalent surface with a Fresnel coefficient equal to the amplitude reflection coefficient of the corresponding smooth plate formed by the mean planes of the boundaries). The assumptions entering into this model are specified in detail as follows:

1. The system consists of an homogeneous and isotropic thin film with complex refractive index and an isotropic substrate. Both ambient-film and film-substrate boundaries are geometrically identical (identical thin film denoted I.T.F afterwards) and generated by a stationary isotropic stochastic process.
2. The height-deviation ζ of the surfaces from their mean planes is characterised by a Gaussian probability density function involving two parameters : the surface RMS height σ, and the correlation length τ.
3. Boundaries are locally smooth (LSRS-type film : see [14] p.254)
4. The incident wave is plane and monochromatic.
5. The dimensions of the irradiated surface (2X, 2Y) are much greater than the wavelength λ of incident light and the surface correlation length τ.
6. The point of observation is in the Fraunhofer diffraction zone.

The paper is arranged as follows:

- Section 2 derives the general and simplified expressions of the amplitude reflection coefficient for a system substrate-identical thin film.
- In Section 3 we evaluate the coherent and incoherent intensities reflected from the system.
- Section 4 specifies the local illumination model.
- Section 5 provides a numerical and a visual estimation of the error committed on the directional-diffuse component by assuming a uniform reflection coefficient in the Helmholtz-Kirchhoff integral.
- Finally, the last section of this contribution presents the conclusions.

2 Amplitude reflection coefficient for a system substrate-identical thin film

The illumination model described by He, Torrance, Sillion and Greenberg in 1991 [8] was obtained by applying the scalar form of the Kirchhoff theory to the case of a single rough surface with uniform reflection coefficient. As it will be shown hereafter, the amplitude reflection coefficient of a system substrate-I.T.F. depends on space coordinates by means of ζ and thus, using the results of He, Torrance, Sillion and Greenberg for this kind of system is inappropriate. The model has to be extended to account for a non uniform reflection coefficient, the expression of which will be derived below.

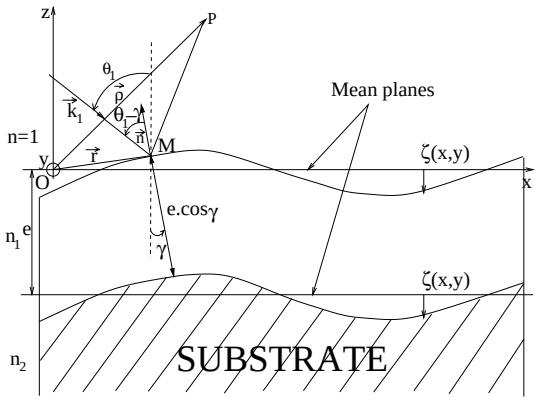

Fig. 1. Identical thin film

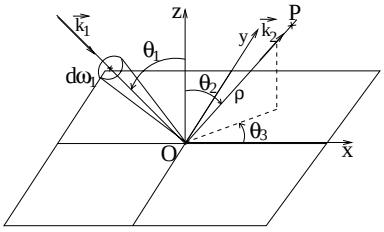

Fig. 2. Incident and scattered waves

2.1 General expression of the reflection coefficient of a system substrate-I.T.F

Consider a plane progressive monochromatic unpolarised wave incident under the angle θ_1 on the upper mean plane of the film (see Fig. 1). This wave shall be resolved into two linearly polarised components, with polarisation planes respectively parallel ($//$) and perpendicular ($\perp$) to the plane of incidence. The film is assumed to be the LSRS type, which allows us to make the tangent plane approximation. The I.T.F. is then represented locally by a plane parallel plate inclined under the angle γ to the (Ox) axis (see Fig. 1). Assuming that the transverse dimensions of this plate are much greater than wavelength, the amplitude of the local electric field can be obtained by summing the amplitudes of the multiple reflected waves, to infinity, for both components of the incident wave. The field reflected by the plate, E_{lsc} is then expressed by means of the following classic equations (see e.g. [9]):

$$E_{lsc} = R_l E_{l\,incident} \quad R_l = \frac{R_{01l} + R_{12l} e^{j\phi}}{1 + R_{01l} R_{12l} e^{j\phi}} \tag{1}$$

where $j^2 = -1$ and subscript l denotes either the parallel or perpendicular ($l = //or\ \perp$) component with:

$$R_{01\perp} = \frac{\cos i - \sqrt{n_1^2 - \sin i^2}}{\cos i + \sqrt{n_1^2 - \sin i^2}} \quad R_{12\perp} = \frac{\sqrt{n_1^2 - \sin i^2} - \sqrt{n_2^2 - \sin i^2}}{\sqrt{n_1^2 - \sin i^2} + \sqrt{n_2^2 - \sin i^2}} \tag{2}$$

$$R_{01//} = \frac{n_1^2 \cos i - \sqrt{n_1^2 - \sin i^2}}{n_1^2 \cos i + \sqrt{n_1^2 - \sin i^2}} \quad R_{12//} = \frac{n_2^2\sqrt{n_1^2 - \sin i^2} - n_1^2\sqrt{n_2^2 - \sin i^2}}{n_2^2\sqrt{n_1^2 - \sin i^2} + n_1^2\sqrt{n_2^2 - \sin i^2}}$$

where:

$$i = \theta_1 - \gamma \quad \phi = \frac{4\pi e}{\lambda} \cos\gamma \sqrt{n_1^2 - \sin i^2}$$

As γ expresses by means of the partial derivatives $\zeta_x^{'} = \partial\zeta/\partial x$ and $\zeta_y^{'} = \partial\zeta/\partial y$ of the random height variable $\zeta(x, y)$ in the form:

$$\cos\gamma = 1/\sqrt{1 + \zeta_x^{'2} + \zeta_y^{'2}}$$

it follows that R_l can also be expressed by means of $\zeta_x^{'}$ and $\zeta_y^{'}$. However, as the general expression of R_l is difficult to integrate in the Helmholtz-Kirchhoff integral (see Section 3), we will use the small-slope assumption, which allows to limit ourselves to a first order expansion of R_l in $\zeta_x^{'}$ and $\zeta_y^{'}$ [13].

2.2 First order expansion of the reflection coefficient

As locally smooth rough surfaces are characterised by small partial derivatives $\zeta_x^{'}$ and $\zeta_y^{'}$, $R_{//}$ and $R_\perp$ (see equations (1) and (2)) can be expanded to the first order in $\zeta_x^{'}$ and $\zeta_y^{'}$ as follows:

$$R_\perp = \alpha_\perp + \beta_\perp \zeta_x^{'} + o(\zeta_x^{'}) + o(\zeta_y^{'}) \quad R_{//} = \alpha_{//} + \beta_{//}\zeta_x^{'} + o(\zeta_x^{'}) + o(\zeta_y^{'})$$

with:

$$\begin{aligned}
\alpha_\perp &= \frac{(K - J_1)(J_1 + J_2) + (K + J_1)(J_1 - J_2)e^{j\phi_0}}{(K + J_1)(J_1 + J_2) + (K - J_1)(J_1 - J_2)e^{j\phi_0}} \\
\alpha_{//} &= \frac{(n_1^2K - J_1)(n_2^2J_1 + n_1^2J_2) + (n_1^2K + J_1)(n_2^2J_1 - n_1^2J_2)e^{j\phi_0}}{(n_1^2K + J_1)(n_2^2J_1 + n_1^2J_2) + (n_1^2K - J_1)(n_2^2J_1 - n_1^2J_2)e^{j\phi_0}} \\
\beta_\perp &= \frac{2I\left[(J_1^2 - K^2)(J_1 + J_2)^2 + (K^2 - J_1^2)(J_1 - J_2)^2 e^{2j\phi_0}\right]}{J_1\left[(K + J_1)(J_1 + J_2) + (K - J_1)(J_1 - J_2)e^{j\phi_0}\right]^2} \\
&\quad + \frac{8IK^2(J_1^2 - J_2^2)(2j\pi e J_2/\lambda - 1)e^{j\phi_0}}{J_2\left[(K + J_1)(J_1 + J_2) + (K - J_1)(J_1 - J_2)e^{j\phi_0}\right]^2}
\end{aligned} \tag{3}$$

$$\beta_{//} = \frac{2n_1^2 I\left[(J_1^2 - K^2)(n_2^2J_1 + n_1^2J_2)^2 + (K^2 - J_1^2)(n_2^2J_1 - n_1^2J_2)^2 e^{2j\phi_0}\right]}{J_1\left[(n_1^2K + J_1)(n_2^2J_1 + n_1^2J_2) + (n_1^2K - J_1)(n_2^2J_1 - n_1^2J_2)e^{j\phi_0}\right]^2}$$

$$+\frac{8n_1^2IK^2[n_1^2n_2^2(J_2^2-J_1^2)+(2j\pi eJ_2/\lambda)(n_2^4J_1^2-n_1^4J_2^2)]e^{j\phi_0}}{J_2\left[(n_1^2K+J_1)(n_2^2J_1+n_1^2J_2)+(n_1^2K-J_1)(n_2^2J_1-n_1^2J_2)e^{j\phi_0}\right]^2}$$

$$\phi_0=\frac{4\pi eJ_1}{\lambda}\quad K=\cos\theta_1\quad I=\sin\theta_1\quad J_i=\sqrt{n_i^2-\sin{\theta_1}^2}\text{,i=1,2}$$

These simplified expressions of $R_\perp$ and $R_{//}$ will be used instead of the full expressions of the reflection coefficient in the Helmholtz-Kirchhoff integral (see next section).

3 Evaluation of the coherent and incoherent intensities

In this section, we derive the expressions of the intensities reflected coherently and incoherently from the system, which are at the basis of our illumination model.

3.1 Field reflected from an ITF in the Fraunhofer diffraction zone

The scalar form of the Helmholtz-Kirchhoff integral [13] applied to both components of the incident wave provides an expression of the electric field diffracted at a point P in the far zone (see Fig. 2), in a direction defined by angles θ_2 and θ_3, as a function of the reflected electric field E_{lsc} and its normal derivative with respect to the normal on the surface S:

$$E_l(P)=\frac{1}{4\pi}\iint_S\left[E_{lsc}\frac{\partial\psi}{\partial n}-\psi\frac{\partial E_{lsc}}{\partial n}\right]dS\quad\psi=\frac{e^{jk\rho-\overrightarrow{k_2}.\overrightarrow{r'}}}{\rho}\quad k=\frac{2\pi}{\lambda}$$

Subscript l denotes either the parallel or perpendicular ($l=//or\ \perp$) component, $\overrightarrow{k_2}$ the wave vector of the scattered wave, ψ the Green function, ρ the distance between the origin of the reference frame and point P, and $\overrightarrow{r'}$ the vector from the origin to a point M on the upper boundary (see Fig. 1 and Fig. 2). The incident plane wave is represented by the scalar electric field $E_{linc}=E_{l0}e^{j(\overrightarrow{k_1}.\overrightarrow{r'}-\omega t)}$ where E_{l0} is the amplitude of the wave, ω is its angular frequency and $\overrightarrow{k_1}$ is the incident wave vector. The time-factor $e^{-j\omega t}$ will be omitted subsequently. The reflected electric field E_{lsc} and its derivative along the normal $\overrightarrow{n}$ at point M then express as:

$$E_{lsc}=R_lE_{l0}e^{j\overrightarrow{k_1}.\overrightarrow{r}}\quad\frac{\partial E_{lsc}}{\partial n}=\left[jR_l\overrightarrow{k_1}.\overrightarrow{n}+\nabla R_l.\overrightarrow{n}\right]E_{linc}$$

For a surface with small partial derivatives ($|\zeta_x'(x,y)|<<1$ and $|\zeta_y'(x,y)|<<1$), it can be proved that the term $\nabla R_l.\overrightarrow{n}$ is negligible with respect to $R_l\overrightarrow{k_1}.\overrightarrow{n}$. It holds then that:

$$E_{lsc}\frac{\partial\psi}{\partial n}-\psi\frac{\partial E_{lsc}}{\partial n}=jR_l(\overrightarrow{v}.\overrightarrow{n})E_{linc}\psi \tag{4}$$

with:

$$\overrightarrow{v}=\overrightarrow{k_1}-\overrightarrow{k_2}\begin{pmatrix}v_x=(2\pi/\lambda)(\sin\theta_1-\sin\theta_2\cos\theta_3)\\ v_y=-(2\pi/\lambda)\sin\theta_2\sin\theta_3\\ v_z=(-2\pi/\lambda)(\cos\theta_1+\cos\theta_2)\end{pmatrix}\qquad\overrightarrow{n}=\frac{1}{\sqrt{1+{\zeta_x'}^2+{\zeta_y'}^2}}\begin{pmatrix}-\zeta_x'\\ -\zeta_y'\\ 1\end{pmatrix}$$

After expanding equation (4) to the first order in $\zeta_x^{'}$ and $\zeta_y^{'}$ and replacing into the Helmholtz-Kirchhoff integral, we obtain:

$$E_l(P) = \frac{-je^{jk\rho}}{2\lambda\rho} E_{l0} \iint_S \left[(\alpha_l v_x - \beta_l v_z)\, \zeta_x^{'} + \alpha_l v_y \zeta_y^{'} - \alpha_l v_z \right] e^{j \overrightarrow{v} . \overrightarrow{r}} dS$$

By analogy with the calculations of Beckmann and Spizzichino, and using the same assumptions, we find:

$$E_l(P) = K \left[F_l \iint_S e^{j \overrightarrow{v} \overrightarrow{r}} dS + \epsilon_l(X,Y) \right] \tag{5}$$

$$\text{with:} \quad K = \frac{-je^{jk\rho}}{2\lambda\rho} E_{l0} \quad F_l = \frac{\lambda}{2\pi} \left(\beta_l v_x - \alpha_l \frac{\overrightarrow{v} . \overrightarrow{v}}{v_z} \right) \tag{6}$$

$$\epsilon_l(X,Y) = \frac{j\lambda}{2\pi v_z} \left[(\alpha_l v_x - \beta_l v_z) \int_{-Y}^{Y} \left[e^{j \overrightarrow{v} \overrightarrow{r}} \right]_{-X}^{X} dy + \alpha_l v_y \int_{-X}^{X} \left[e^{j \overrightarrow{v} \overrightarrow{r}} \right]_{-Y}^{Y} dx \right]$$

where S is the illuminated part of the surface. Beckmann and Spizzichino label the term $\epsilon_l(X,Y)$ "edge effects", as it involves values of $\overrightarrow{v} . \overrightarrow{r}$ at the surface edges and neglect it in the calculation of the coherent component of the electric field, given that the dimensions of the surface are much greater than wavelength. It can nevertheless be shown that despite this assumption, the edge effects are negligible only close to the specular direction. However, making one further assumption ([12] p.86), it is possible to evaluate the average of the edge terms. It should be pointed out that if we take $\beta = 0$, equations (5)-(6) amount to the results found by Beckmann et Spizzichino in the case of a single rough surface ([1] p.28).

3.2 Coherent intensity

From equation (5), we draw the expression of the average intensity $I_{l\,c}$ of the field coherently reflected from the whole surface at point P. If we label $\bar{E}_l(P)$ the conjugate of the electric field $E_l(P)$ and $\langle E_l(P) \rangle$ the average of $E_l(P)$ with respect to the statistical variable, we obtain:

$$I_{l\,c} = \frac{\rho^2}{A \cos\theta_2} \langle E_l(P) \rangle \left\langle \bar{E}_l(P) \right\rangle$$

with:

$$\langle E_l(P) \rangle = K \left[F_l \left\langle \int_{-X}^{X} \int_{-Y}^{Y} e^{j \overrightarrow{v} . \overrightarrow{r}} dx\, dy \right\rangle + \langle \epsilon_l(X,Y) \rangle \right]$$

$$\left\langle \int_{-X}^{X} \int_{-Y}^{Y} e^{j \overrightarrow{v} \overrightarrow{r}} dx dy \right\rangle = A \sin_c(v_x X) \sin_c(v_y Y) \chi_1(v_z)$$

$$\langle \epsilon_l(X,Y) \rangle = \frac{\lambda A}{2\pi} \left(\alpha_l \frac{v_x^2 + v_y^2}{v_z} - \beta_l v_x \right) \sin_c(v_x X) \sin_c(v_y Y) \chi_1(v_z)$$

where χ_1 is the one-dimensional characteristic function of the rough surface and:

$$\sin_c(x) = \frac{\sin(x)}{x}, x \in \Re.$$

This implies, after some simplifications:

$$\langle E_l(P) \rangle = \frac{j e^{j k \rho}}{4\pi\rho} \alpha_l A v_z \sin_c(v_x X) sin_c(v_y Y) \chi_1(v_z) E_{l0}$$

For a surface with a Gaussian height distribution, characterised by the probability density function $p(\zeta) = \frac{1}{\sigma\sqrt{2\pi}} e^{-\zeta^2/2\sigma^2}$, we have:

$$\chi_1(v_z) = \frac{1}{\sigma\sqrt{2\pi}} \int_{-\infty}^{\infty} e^{-\zeta^2/2\sigma^2} e^{j v_z \zeta} d\zeta = e^{-g/2}$$

with $g = (\sigma v_z)^2$. The coherent intensity then becomes:

$$I_{l\,c}(\theta_1, \theta_2, \theta_3) = \frac{A|\alpha_l|^2}{4\lambda^2 \cos\theta_2} \left[\sin_c(v_x X) \sin_c(v_y Y)\right]^2 (\cos\theta_1 + \cos\theta_2)^2 e^{-g} I_{l\,inc} d\omega_1$$

where $I_{l\,inc}$ represents the incident intensity for the parallel or perpendicular component and $d\omega_1$ the incident solid angle. It should be noted that in the case when $X >> \lambda$ and $Y >> \lambda$, the coherent intensity is zero in all directions, excepted in the specular direction. In this case the coherent intensity will be identified with the specular intensity of our illumination model (see Section 4). For unidirectional incidence with solid angle $d\omega_1$, the specular intensity becomes (see [8] p. 186):

$$I_{l\,sp}(\theta_1, \theta_2) = |\alpha_l|^2 e^{-g} \Delta I_{l\,inc} \tag{7}$$

Δ is a function which is unity in the specular cone of reflection and zero otherwise. We have to notice that formula (7) does not involve β_l: the specular intensity reflected by the system substrate-I.T.F. is equal to the specular intensity reflected by an equivalent surface with a Fresnel factor equal to the reflection coefficient of the corresponding smooth film (the parallel plate formed by the mean planes of the boundaries).

3.3 Incoherent intensity

The incoherent (or directional-diffuse $I_{l\,dd}$) intensity is given by the formula:

$$I_{l\,dd} = \frac{\rho^2}{A\cos\theta_2} \left(\left\langle E_l(P) \bar{E}_l(P) \right\rangle - \langle E_l(P) \rangle \left\langle \bar{E}_l(P) \right\rangle \right)$$

This expression can be developed using the one-dimensional (χ_1) and two-dimensional (χ_2) characteristic functions of the surface (see [12] p. 17). Assuming that the edge effects are non stochastic (so that they give no contribution to the incoherent intensity) we obtain:

$$I_{l\,dd} = \frac{\rho^2 |K F_l|^2}{A\cos\theta_2} \left(\int_{-X}^{X} \int_{-Y}^{Y} \int_{-X}^{X} \int_{-Y}^{Y} e^{j(v_x(x-x') + v_y(y-y'))} \chi_2(v_z, -v_z, \rho) dx dy dx' dy' \right.$$

$$-\int_{-X}^{X}\int_{-Y}^{Y}\int_{-X}^{X}\int_{-Y}^{Y} e^{j(v_x(x-x')+v_y(y-y'))}\chi_1(v_z)\chi_1(-v_z)dxdydx'dy'\Bigg)$$

For a Gaussian height distribution, the final formula for the directional-diffuse intensity is:

$$I_{l\,dd} = \frac{\pi\tau^2}{4\lambda^2\cos\theta_2}\left|\beta_l\hat{v}_x - \alpha_l\frac{\overrightarrow{\hat{v}}\,.\,\overrightarrow{\hat{v}}}{\hat{v_z}}\right|^2 e^{-g}\sum_{m=1}^{\infty}\frac{g^m}{mm!}e^{-\frac{\pi^2\tau^2(\hat{v}_x^2+\hat{v}_y^2)}{m\lambda^2}}I_{l\,inc}d\omega_1 \qquad (8)$$

where τ is the correlation length of the surface and $\overrightarrow{\hat{v}} = \overrightarrow{v}/\|v\|$.
It should be noted that taking $\beta_l = 0$ in equation (8) leads to the formula of the directional-diffuse intensity given by He, Torrance, Sillion and Greenberg ([8] p.186) excepted that the Fresnel factor is replaced by the reflectivity $|\alpha_l|^2$ of the plane parallel plate formed by the mean planes of the surfaces.

4 Local illumination model

Like the model of He, Torrance, Sillion and Greenberg, our illumination model is presented as a sum of three terms : specular intensity, directional-diffuse intensity and uniform-diffuse intensity:

$$I_r(\theta_1,\theta_2,\theta_3) = I_{ud}(\theta_1) + I_{sp}(\theta_1,\theta_2) + I_{dd}(\theta_1,\theta_2,\theta_3) \qquad (9)$$

$I_{sp}(\theta_1,\theta_2)$ is the specular intensity given by formula (7), $I_{dd}(\theta_1,\theta_2,\theta_3)$ is the directional diffuse (see formula (8)) intensity, and $I_{ud}(\theta_1)$ is the uniform diffuse intensity which results from the multiple surface and subsurface reflections and can be approximated by the Lambert formula: $I_{ud}(\theta_1) = |\alpha_l|^2\cos\theta_1 d\omega_1$, where α_l is the zero-order term of the expansion of the reflection coefficient for the parallel or perpendicular component (see formula (3)). The local illumination model for N finite solid angle sources, accounting for both polarisation components is given by:

$$\begin{aligned} I_r(\lambda) &= \sum_{k=1}^{N}\left(|\alpha_k|^2\cos\theta_{1\,k}d\omega_k + |\alpha_k|^2 e^{-g_k}S\Delta\right)I_{inc\,k} \\ &+ \frac{\pi\tau^2 S}{4\lambda^2\cos\theta_2}\sum_{k=1}^{N}|\beta_k|^2 e^{-g_k}\sum_{m=1}^{\infty}\frac{g_k^m}{mm!}e^{-\frac{\pi^2\tau^2(\hat{v_x}^2+\hat{v_y}^2)_k}{m\lambda^2}}I_{inc\,k}\,d\omega_k \end{aligned}$$

where subscript k denotes the k^{th} light source, S is the shadowing function (see [8] equations (23)-(25)) and $I_{inc\,k}$ is the total (parallel + perpendicular) incident intensity for light source k. The terms inside the brackets respectively correspond to the three terms in equation (9) and:

$$|\alpha_k|^2 = \frac{|\alpha_{//_k}|^2 + |\alpha_{\perp k}|^2}{2}$$

$$|\beta_k|^2 = \frac{|\beta_{//}\hat{v}_x - \alpha_{//}(\overrightarrow{\hat{v}}\,.\,\overrightarrow{\hat{v}}/\hat{v}_z)|_k^2 + |\beta_\perp\hat{v}_x - \alpha_\perp(\overrightarrow{\hat{v}}\,\overrightarrow{\hat{v}}/\hat{v}_z)|_k^2}{2}$$

5 Estimation of the error committed on the directional-diffuse component by assuming a uniform reflection coefficient

We have just seen that the first order term in the expansion of the reflection coefficient, β_l, only appeared in the directional-diffuse (incoherent) part of the reflected light. Neglecting this term (which amounts to considering the film as an equivalent surface with a reflection coefficient equal to the amplitude reflection coefficient of the plane parallel plate formed by the mean planes of the I.T.F.) will thus result in an error only on the directional-diffuse term. The next section aims at evaluating this error both numerically and visually according to the angular (θ_1,θ_2 and θ_3) and film (RMS height σ, correlation length τ, thickness e) parameters.

5.1 Directional-diffuse intensity obtained by considering the reflection coefficient to be uniform

A first approximation consists in using the formula given by He, Torrance, Sillion and Greenberg for a rough surface to compute the directional-diffuse intensity reflected in the direction (θ_2, θ_3) (see [8] p.186) by replacing the Fresnel coefficient $|F|^2$ by the reflectivity $|\alpha|^2$ of the plane parallel plate formed by the mean planes of the I.T.F. (which amounts to taking $\beta = 0$ in equation (8)). The directional-diffuse intensity (without shadowing) is then (see Fig. 1 and Fig. 2 for the notations):

$$I_{dd1} = \frac{\pi\tau^2 e^{-g}}{4\lambda^2 \cos\theta_2} \frac{|\alpha_{//}|^2 + |\alpha_\perp|^2}{2} \left(\frac{\overrightarrow{\hat{v}}\,\overrightarrow{\hat{v}}}{\hat{v}_z} \right)^2 \sum_{m=1}^{\infty} \frac{g^m}{mm!} e^{-\frac{\pi^2\tau^2(\hat{v}_x^2+\hat{v}_y^2)}{m\lambda^2}} I_{inc} d\omega_1 \quad (10)$$

5.2 Directional-diffuse intensity obtained by means of a first order expansion of the reflection coefficient.

Using a first order expansion of the reflection coefficient, the total directional-diffuse intensity was obtained in the form (see equation (8)):

$$I_{dd2} = \frac{\pi\tau^2 e^{-g}}{4\lambda^2 \cos\theta_2} \frac{|\beta_{//}\hat{v}_x - \alpha_{//}(\overrightarrow{\hat{v}}\,\overrightarrow{\hat{v}}/\hat{v}_z)|^2 + |\beta_\perp \hat{v}_x - \alpha_\perp(\overrightarrow{\hat{v}}\,\overrightarrow{\hat{v}}/\hat{v}_z)|^2}{2} \cdot \frac{}{\sum_{m=1}^{\infty} \frac{g^m}{mm!} e^{-\frac{\pi^2\tau^2(\hat{v}_x^2+\hat{v}_y^2)}{m\lambda^2}} I_{inc} d\omega_1} \quad (11)$$

5.3 Numerical estimation of the error

The relative error committed by using I_{dd1} instead of I_{dd2} for the directional-diffuse intensity is evaluated by the function D which depends on wavelength, incidence angle θ_1 and viewing angles θ_2 and θ_3:

$$D(\lambda, \theta_1, \theta_2, \theta_3) = \frac{I_{dd2} - I_{dd1}}{I_{dd2}}$$

$$D = \frac{\left| \beta_{//}\hat{v}_x - \alpha_{//}\frac{\overrightarrow{\hat{v}}\,\overrightarrow{\hat{v}}}{\hat{v}_z} \right|^2 + \left| \beta_\perp \hat{v}_x - \alpha_\perp \frac{\overrightarrow{\hat{v}}\,\overrightarrow{\hat{v}}}{\hat{v}_z} \right|^2 - \left| \alpha_{//}\frac{\overrightarrow{\hat{v}}\,\overrightarrow{\hat{v}}}{\hat{v}_z} \right| - \left| \alpha_\perp \frac{\overrightarrow{\hat{v}}\,\overrightarrow{\hat{v}}}{\hat{v}_z} \right|}{\left| \beta_{//}\hat{v}_x - \alpha_{//}\frac{\overrightarrow{\hat{v}}\,\overrightarrow{\hat{v}}}{\hat{v}_z} \right|^2 + \left| \beta_\perp \hat{v}_x - \alpha_\perp \frac{\overrightarrow{\hat{v}}\,\overrightarrow{\hat{v}}}{\hat{v}_z} \right|^2}$$

It shall be noticed that D is independent of the surface parameters σ and τ. In order to

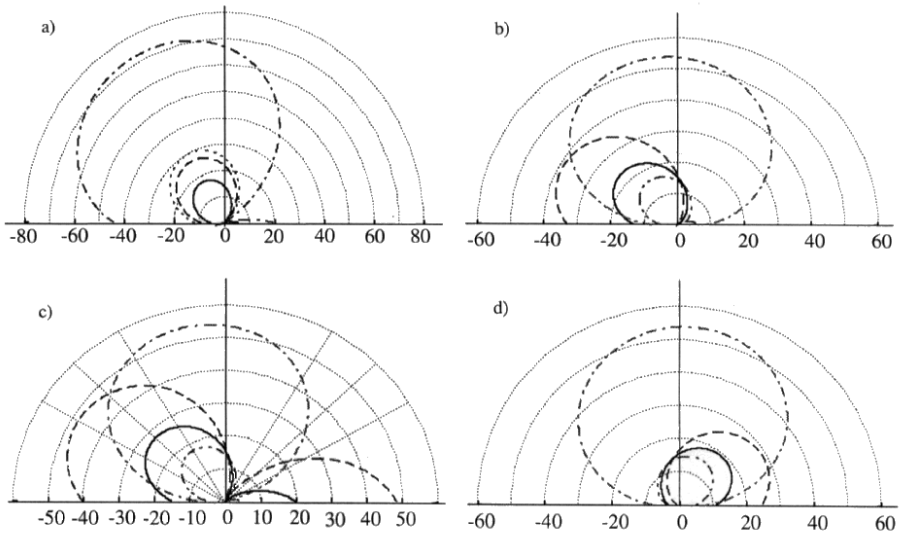

Fig. 3. a) Relative error for $\theta_1 = 60°$, $\theta_3 = 0°$ and for the four Meyer wavelengths:
—— 631.4 nm ····· 557.7 nm - - - 490.9 nm -·-·- 456.4 nm
b) c) d) Relative error for: $b)\theta_3 = 50°$ $c)\theta_3 = 0°$ $d)\theta_3 = 110°$
The four polar curves correspond to different values of the angle of incidence:
– – – θ_1=30° —— θ_1=45° -·-·-θ_1=60° -·-·- θ_1=80°

estimate this error, we made a series of numerical simulations. The error was estimated for an I.T.F. of copper oxide (thickness $e = 800nm$) on a copper substrate. Figure 3a-d are polar representations of the relative error D as a function of the viewing angle θ_2 (the polar radius is D and the polar angle θ_2). Figure 3a displays the variations of D for an angle of incidence $\theta_1 = 60°$, in the plane of incidence ($\theta_3 = 0°$), for the four Meyer wavelengths [11]. It can be noticed that the error on the component with $\lambda = 631.4nm$ is quite small ($D = 18$ percent) whereas it is very important for the component with $\lambda = 456.4nm$ (about 73 percent). Similarly, the polar plots on Figures 3b,c,d represent the variations of the relative error in different viewing planes (characterised by angle θ_3) for several values of the angle of incidence θ_1 and for the red ($\lambda = 631.4nm$) component. It can be seen that the maximum value of the error strongly depends on the value of the incidence angle. For instance, in the plane of incidence (see Fig. 3b) the maximum of the error is 18 percent for $\theta_1 = 60°$ and 55 percent for $\theta_1 = 80°$. Note that the error is equal to zero for some values of the angle θ_2, which correspond to $v_x = 0$. As a conclusion, we can state that for given incidence and viewing angles, the relative error may be quite important, depending on the wavelength of light, and for a given wavelength and given viewing angles, the error can become very significant according to the angle of incidence of light.

5.4 Visualisation of the error

We have just seen that the relative error on the diffuse component was independent of the surface parameters (RMS height σ and correlation length τ) and could be great for some values of the angular parameters. The aim of this section is to appraise visually the difference between pictures rendered by both models according to the surface parameters.

The following pictures (see Appendix), generated by a spectral ray-tracing algorithm working on the four Meyer [11] wavelengths, display the evolution of the directional-diffuse component of light reflected by a system substrate-identical thin film according to the film parameters (correlation length τ, RMS height σ, film thickness). The spheres are made of a thin identical copper oxide film on a copper substrate (excepted for pictures 5c and 5f where the substrate is silver). The materials are characterised by their complex refractive indices, derived from experimental data for each one of the four Meyer wavelengths. The film spreading on the spheres was simulated by means of a sinusoidal variation of thickness from e_{max} at the top of the sphere to e_{min} at the bottom. Pictures 4-6 a, b, c were obtained by the use of formula (10) for the directional-diffuse intensity, whereas pictures 4-6 d, e, f were rendered by means of formula (11). The lighting consists of a single spherical light source situated behind the observer. It can be noticed that the visual differences between pictures rendered by the two models can be significant or negligible depending on the value of the film parameters. For instance there is a clear difference between pictures 4a and 4d: Fig. 4d displays a wider diffuse spot and a green fringe of interference which does not appear on figure 4a. As the correlation length increases with σ fixed at $100nm$ (see Fig. 4b and 4d), the surface becomes smoother with respect to the incident light, and the differences between the two pictures vanish (it can be noticed that the diffuse patch is smaller than on figures 4a and 4d: the surface becomes less diffuse as σ/τ decreases). Similarly, as the RMS height σ increases from $100nm$ to $130nm$ with τ fixed at $1.6\mu m$ (see figures 4c and 4f) the diffuse term spreads out slightly, but the visual differences between the two pictures remain small. Pictures 5a-f show the directional-diffuse term with σ and τ fixed at $100nm$ and $1\mu m$ respectively, for different values of the oxide film thickness, on a copper (5a,5b,5d,5e) or silver (5c,5f) substrate. It can be noted that whatever the thickness of the oxide film, pictures rendered by both models are quite different for such values of σ and τ. If now the ratio σ/τ is held constant at 0.1 (see figures 6a-f), increasing σ tends to attenuate the differences between pictures rendered by both models. As a conclusion, we can state that the influence of the surface parameters on the visual difference between the two models is clear: for given illumination and viewing angles, a visual difference which is not important can become significant for some values of the surface parameters.

Pictures 7a-d and 8 display scenes rendered by a full semi-global illumination model obtained by completing the local illumination model (see Section 4) by global reflection and transmission terms. Pictures 7a, 7b, 7c, 7d represent a piece of oxidised copper (Fig. 7a and 7b) or iron (Fig. 7c and 7d) piping illuminated by two spherical light sources. The thickness of the oxide film was taken to be a function of the space variables varying between 500 and $1000nm$. Pictures 7a and 7c were obtained by using formula (11) for the directional diffuse intensity whereas for pictures 7b and 7d, formula (10) was used. It can be noticed that on Fig. 7a, the yellow fringe is wider than on Fig. 7b, which exhibits a bigger green fringe of interference. The difference between Fig. 7c and Fig. 7d is less obvious, but the fringes seem brighter on Fig. 7c and the green interference fringe wider on Fig. 7d. The global reflection of the walls can be clearly observed on the iron piping.

Figure 8 depicts a set of saucepans made of an iron substrate coated with an iron oxide I.T.F.. The thickness of the oxide film on the discs forming the bottom of each saucepan is bounded by the values e_{min} and e_{max} (different for each saucepan) and increases irregularly from e_{min} at the centre of the disc to e_{max} at its edge. The reflection of the yellow table can be seen in the bottom of the saucepans. Computation times are similar to those obtained by any classic ray-tracing algorithm and quite identical for the two models. For instance rendering picture 7.b takes about half an hour for a resolution of 900x600, on a Pentium II 333 Mhz, whereas rendering Fig. 7a only takes 11 per cent more computation time.

6 Conclusions and future directions

We have presented a new illumination model for substrate-identical thin film-type systems. Based on scalar diffraction theories, it allows to evaluate with given accuracy the components of light reflected from a system substrate-identical thin film. We have shown both numerically and visually the consistency of this model by comparison with a simple classic approach. Future work consists in expanding this illumination model to account for systems of the kind substrate-general thin film (film with mutually independent rough boundaries) and to rough multilayer systems.

References

1. Beckmann, P., Spizzichino, A., "The Scattering of Electromagnetic Waves from Rough Surfaces", Pergamon Press, 1963.
2. Born, M. and Wolf, E, 1964, Principles of Optics (Pergamon Press, Oxford).
3. Callet, P., "Interférences, couches minces et peintures métallisées", International Journal of CADCAM and Computer Graphics, vol. 9, pp 251-264, Paris, 1994, Hermes.
4. Callet, P., "Couleur-lumière Couleur-matière", Diderot Editeur, Arts et Sciences, 1998.
5. Cook, R. L. and Torrance, K. E., "A Reflectance Model for Computer Graphics", ACM transactions on Graphics, 1, 1982, pp. 7-24.
6. Godlewski, J., Kalinowski, S., Davoli, I. and Bernardini, R., 1987, Thin Solid Films vol. 146, 115.
7. Gondek, J. S., Meyer, G. W, Newman, J.G., "Wavelength Dependent Reflectance Functions". Proceedings of Siggraph'94. In Computer Graphics.
8. He, X. D, Torrance, K. E., Sillion, F. X., Greenberg, D. P., "A Comprehensive Physical Model for Light Reflection", Computer Graphics, Vol. 25, N. 4, 1991.
9. Hecht, E., 1987, Optics, 2nd Edition, Adison-Wesley Publishing Co.
10. Icart, I. and Arquès, D., "An Approach to geometrical and Optical Simulation of Soap Froth", Computers & Graphics vol 23:3, Elsevier Science, 1999.
11. Meyer, G. W., "Wavelength Selection for Synthetic Image Generation", Computer Vision, Graphics and Image Processing, vol. 41, 57-59, 1988.
12. Ogilvy, J. A., "Theory of Wave Scattering from Random Rough Surfaces", Institute of Physics Publishing, Bristol and Philadelphia.
13. Ohlidal, I. and Lukes, F., "Ellipsometric parameters of rough surfaces and of a system substrate-thin films with rough boundaries", 0pt. Commun. 5, 1972.
14. Ohlidal, I., Navratil, K., "Scattering of light from multilayer systems with rough boundaries", Progress in Optics, Vol. 34, Elsevier Science B.V, 1995.
15. Szczyrbowski, J., Dietrich, A. and Hoffmann H., 1982, Phys. Status Solidi a 69, 217.